Check for updates

Macromolecular Materials and Engineering
www.mme-journal.de

Interfacial Fabrication of CNTs/PVDF Bilayer Actuator with Fast Responses to the Light and Organic Solvent Vapor Stimuli

Gui Zhang, Luke Yan, Lingtong Ji, Chaohui Liu, Lei Zhang,* Wei Zhang, Yujing Nie, Peng Xiao, and Tao Chen**

A multiple stimuli-responsive actuator with an ability of rapid and sensitive responding is highly desirable for the development of biomimetic actuation applications. Herein, a bilayer actuator with fast and sensitive responses to acetone vapor and light stimuli is reported based on polyvinylidene fluoride (PVDF) membrane with a hierarchical porosity and macroscopic carbon nanotubes (CNTs) assembled film. The CNTs film with uniform and tunable thickness is prepared by a macroscopic interfacial assembly strategy and transferred integrally onto the PVDF membrane. Under the infrared light, this CNTs/PVDF bilayer actuator can bend rapidly within 1 s and generate large stress. Moreover, for the acetone vapor stimuli, the actuator bends within 0.19 s and also reverses in 1.24 s to the initial state, showing sensitive and fast responses to acetone stimuli, as well as outstanding stability and repeatability.

Recently, multistimuli responsive actuators have been developed by virtue of soft polymer materials and functional inorganic nanomaterials, to mimic biological systems possessing heterogeneous mechanical properties.[1,2] These kinds of actuators can convert external stimuli such as light,[3] heat,[4,5] electrical,[6] and organic vapors[7] to mechanical energy and show reversible dimension changes. To achieve controllably actuation, it is significant to integrate the active materials with assistant inertia materials.[8] A simple bilayer structure is usually adapted to combine actuation layer with an inert layer in a synergistic manner. The actuation is mostly caused by the difference in the volume expansion or contraction of two layers. For example, carbon nanomaterials like carbon nanotube (CNT), graphene serve as joule/photothermal conversion materials that can be employed to fabricate electrical or photodriven actuators.[9] Combining with these carbon nanomaterials, some responsive polymer such as cellulose,[10] polyvinylidene fluoride (PVDF),[11] or polypropylene[12] are further used to construct multistimuli responsive actuators that response to solvent vapors, light, and electrical stimuli.

To date, many actuators consisting of carbon nanomaterials and polymer layer still display slow responses (tens of seconds to a few minutes) and insufficient sensitivity in the actuation/recovery process triggered by solvent vapors and[7,13,14] light stimuli.[15–19] Zhang et al.[20] and Deng et al.[21] reported respectively thermally and solvent responsive actuators with bilayer CNT/polyethylene composite, and graphene/epoxy-based polymer. These actuators can be bent reversibly in water or acetone under the controlled of thermal and near-infrared light. But their response speed is slow in the order of several minutes. To improve the reversible response rate, the composite film actuators with thin thickness are prepared. Qu et al. reported a graphene oxide/cellulose acetate membrane actuator with a thickness of 140 μm, which bends completely to the acetone vapor within 19 s and recovers within 38 s in air.[7] Leeladhar and Singh prepared a graphene-poly(dimethylsiloxane)/gold bilayer actuator with 55 μm thickness for photo- and chemical vapor-driven soft grippers opens fully within 8 s.[22] However, these thin-film actuators are subjected to apparent fatigue and weak mechanical strength. Increasing the interaction area between actuator and stimuli can enhance rapid response ability. Zhang et al.[23] reported a PVDF/PVA actuator with microchannel patterns that allowed the actuator response rapidly to the acetone gas. The reversible actuation process was still slow and was completed within 6 s. The interaction

G. Zhang, Prof. L. Yan, L. T. Ji, C. H. Liu, Prof. T. Chen
Polymer Materials and Engineering Department
School of Materials Science and Engineering
Chang'an University
Xi'an 710064, P. R. China
E-mail: lkyan@chd.edu.cn; tao.chen@nimte.ac.cn

Prof. L. Zhang, W. Zhang, Dr. P. Xiao, Prof. T. Chen
Key Laboratory of Bio-Based Polymeric Materials Technology and Application of Zhejiang Province
Ningbo Institute of Materials Technology and Engineering
Chinese Academy of Sciences
Ningbo 315201, P. R. China
E-mail: zhanglei@nimte.ac.cn

Prof. Y. Nie
College of Chemistry
Chemical Engineering and Environment
Minnan Normal University
Zhangzhou 363000, P. R. China

The ORCID identification number(s) for the author(s) of this article can be found under https://doi.org/10.1002/mame.202000502.

DOI: 10.1002/mame.202000502

 © 2020 Wiley-VCH GmbH

between PVDF and vapor occurs mainly on the surface and permeation of acetone molecules into PVDF is hindered, leading to insufficient volume expansion and slow response to the vapor stimuli. On another hand, the CNT or graphene layer is usually difficult to coat uniformly on the PVDF membrane by conventional solution casting method,[24] especially in large scale preparation. This will affect the synergistic effects of the actuation layers and resulting controllable actuating deformation.[25] Thus, it is highly desirable to develop effective methods to prepare high-performance actuators that can respond rapidly and sensitively to multiple stimuli. Previously, the carbon-based polymer composites actuators are mainly composed of uniform polymer film or with some surface pattern. There are no work to study the effects of porosity of the polymer film on the actuation performance under the control of light/chemical solvent stimuli.

In present work, we report a robust strategy of fabricating a bilayer actuator with fast and sensitive responses to the acetone vapor and light stimuli. This actuator consists of hierarchically porous PVDF membrane and macroscopic CNTs assembled thin film with uniform thickness. The CNT film was prepared by air/water macroscopic interfacial assembly and can transfer integrally on a porous PVDF film by one-step. Due to the hierarchical porous structures of PVDF and uniform CNT film, this CNTs/PVDF bilayer actuator shows sensitive and fast responses to acetone and light stimuli. Meanwhile, under the acetone gas stimuli, the actuator approaches rapidly to the equilibrate state within 0.2 s and returns to the original state within 1.24 s. The actuator also has stable actuation performance in the cycles of acetone and light stimuli, exhibiting outstanding stability and repeatability.

The fabrication strategy is illustrated in **Figure 1**a. Viscous PVDF/*N*,*N*-dimethylformamide (DMF) mixture is casted on the glass plate by blade casting method before immersing into the water bath (Figure 1a-I,II). Based on the solvent exchanging of DMF/water, phase conversion occurs in the casted PVDF/DMF mixture (Figure 1a-III), leading to a porous PVDF membrane after drying (Figure 1a-IV). Subsequently,

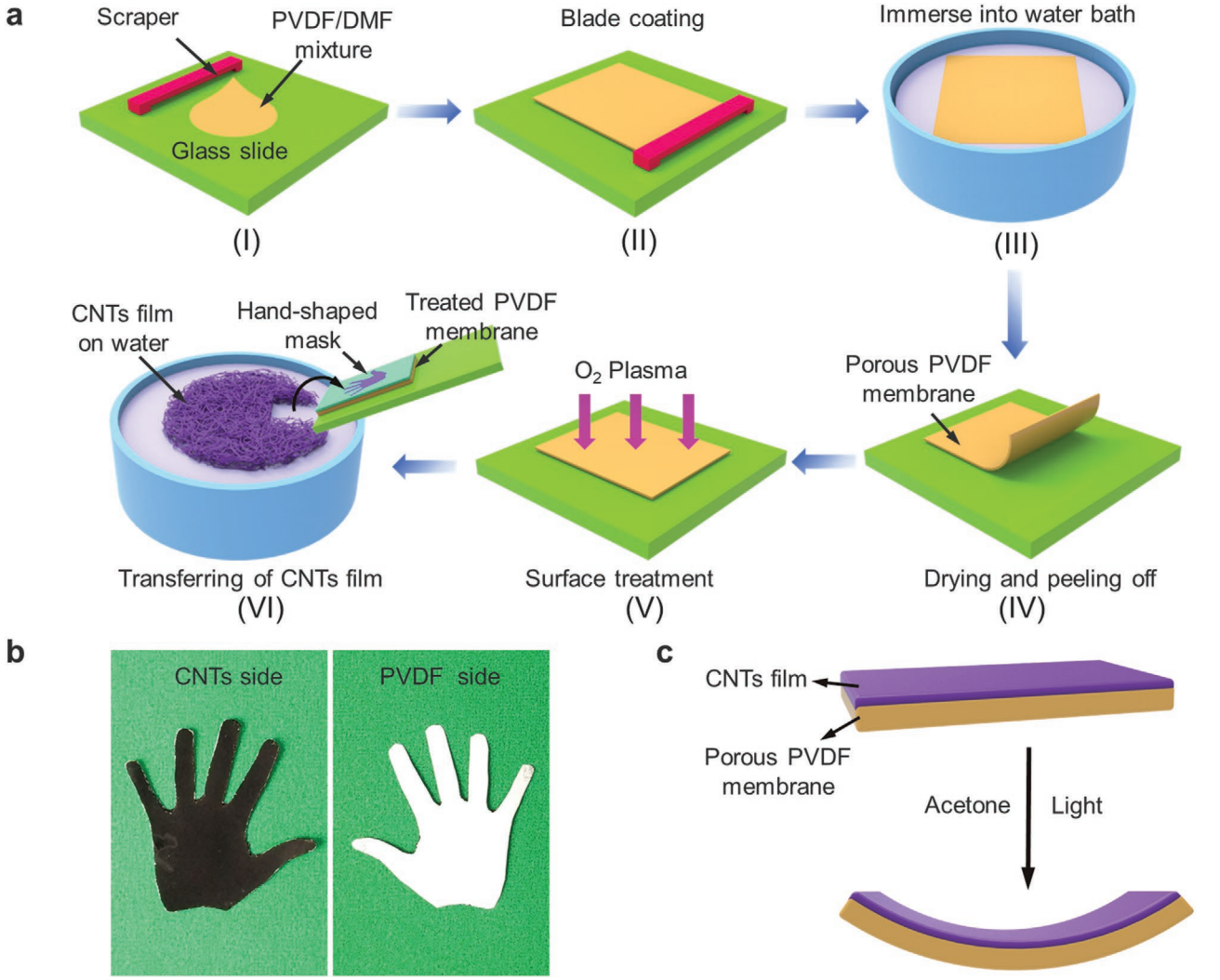

Figure 1. a) Schematic illustration of preparation of the CNTs/PVDF composite membrane. b) Both sides of a hand-shaped CNTs/PVDF composite. c) Responses of CNTs/PVDF bilayer actuator to light and acetone vapor stimuli.

© 2020 Wiley-VCH GmbH

14392054, 2021, 1, Downloaded from https://onlinelibrary.wiley.com/doi/10.1002/mame.202000502 by Ningbo Institute Of Materials, Wiley Online Library on [12/09/2023]. See the Terms and Conditions (https://onlinelibrary.wiley.com/terms-and-conditions) on Wiley Online Library for rules of use; OA articles are governed by the applicable Creative Commons License

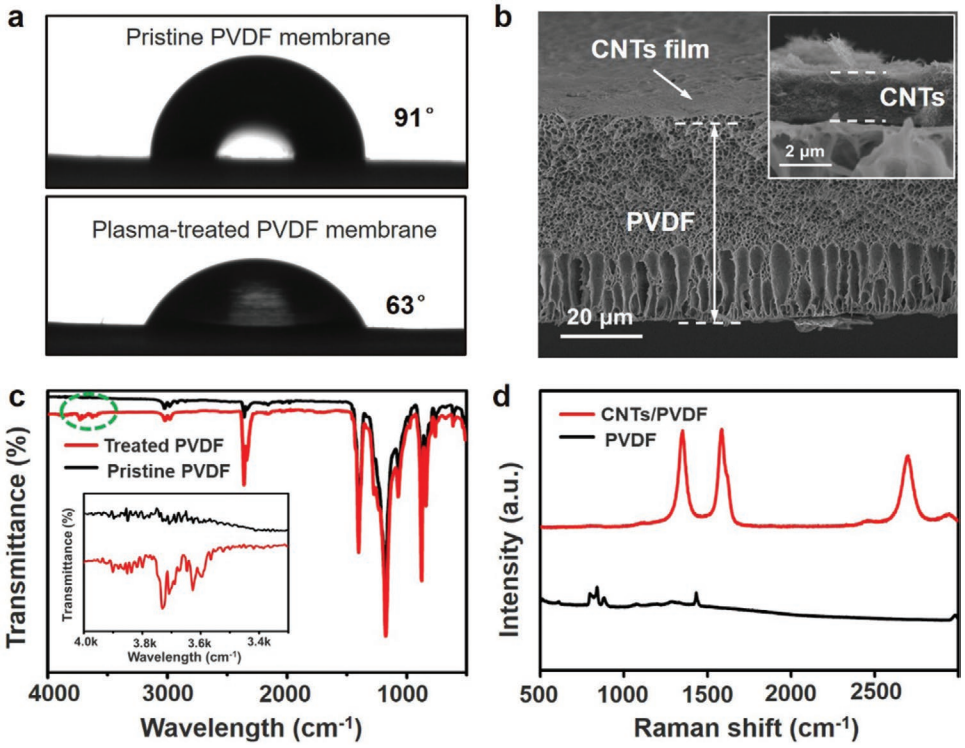

Figure 2. a) Water contact angles of the pristine (91°) and plasma-treated PVDF (63°) membrane. b) SEM image of a CNTs/PVDF composite membrane. c) ATR-FTIR spectra of pristine PVDF membrane (black line) and plasma-treated PVDF membrane (red line). The inset is an enlarged view of the circled area. d) Raman spectra of the PVDF and CNTs/PVDF composite membrane.

one side of the porous PVDF membrane is treated by oxygen plasma to favor the transferring of CNTs film (Figure 1a-V). Previously, we reported a macroscopic freestanding CNTs network film with outstanding mechanical strength by air/water interfacial assembly.[26] This CNTs film can be transferred stably onto the plasma-treated PVDF membrane from water solution surface. In the transferring process of CNTs film (Figure 1a-VI), a hand-shaped mask is employed to cover the PVDF membrane before dipping into the water solution with CNTs film floating on the surface (Figure 1a-VI). The slantly held PVDF/mask is lifted vertically from the bottom of the floating CNTs film. A hand-shaped CNTs film is formed on the PVDF member after removing the mask. The CNTs thin film only attaches to the one side of PVDF membrane, forming an asymmetrical structure (Figure 1b). The resultant bilayer CNTs/PVDF composite membrane can be used as an actuator that responds to multiple stimuli such as light and acetone (Figure 1c).

Due to the inherent hydrophobic surface of the PVDF membrane, CNTs film floating on aqueous solution is incapable of integrally transferring on the PVDF membrane. A protocol of oxygen plasma treatment is performed to change the surface wettability of PVDF membrane. After oxygen plasma treatment, the surface water contact angles (WCAs) of PVDF layer change from 91° to 63° (**Figure 2**a), showing good hydrophilicity. The oxygen plasma treatment can trigger the carbon etching and/or oxidation and defluorination reaction at the surface of PVDF membrane, and incorporate oxygen (CO groups) onto the surface.[27] These changes make the PVDF membrane surface become more hydrophilic.[28] The microstructures of the CNT/PVDF membrane was further observed by scanning electron microscopy (SEM) (Figure 2b). A layer of CNTs film network with uniform thickness of 2 μm attach firmly on PVDF membrane, forming a bilayer structure. The CNTs network film has a nanoscale porosity while the PVDF membrane displays hierarchical pore structures consisting of finger-liked pores and irregular microscopic pores coexisting inside PVDF membrane. The finger-liked pores and irregular microscopic pores distribute separately on two sides of the PVDF membrane, leading to an asymmetrical porous membrane.

The surface composition of oxygen plasma-treated PVDF membrane was examined with attenuated total reflectance-Fourier transform infrared (ATR-FTIR) spectroscopy. Both pristine PVDF membrane and plasma-treated PVDF membrane display characteristic absorption bands of PVDF crystalline phases (α and β phase).[29] The featured peaks around 885 cm^{-1} corresponds to C–H rocking/C–F asymmetrical stretching and the peaks around 1171 and 1402 cm^{-1} are ascribed to the C–F stretching vibrations.[30,31] In comparison to the pristine PVDF membrane, treated PVDF membrane has significant peaks between 3500 and 3800 cm^{-1} (red line in Figure 2c),[32,33] indicating the incorporation of hydroxyl groups on the treated PVDF membrane. In addition, the composition of CNTs/PVDF composite and pure PVDF membranes are also characterized by Raman spectra (Figure 2d). The characteristic D, G, and D bands of CNTs are marked at about 1351, 1585, and 2699 cm^{-1}, respectively,[34,35] which suggests that the CNTs are attached to PVDF in the CNTs/PVDF composite.

© 2020 Wiley-VCH GmbH

14392054, 2021, 1, Downloaded from https://onlinelibrary.wiley.com/doi/10.1002/mame.202000502 by Ningbo Institute Of Materials, Wiley Online Library on [12/09/2023]. See the Terms and Conditions (https://onlinelibrary.wiley.com/terms-and-conditions) on Wiley Online Library for rules of use; OA articles are governed by the applicable Creative Commons License

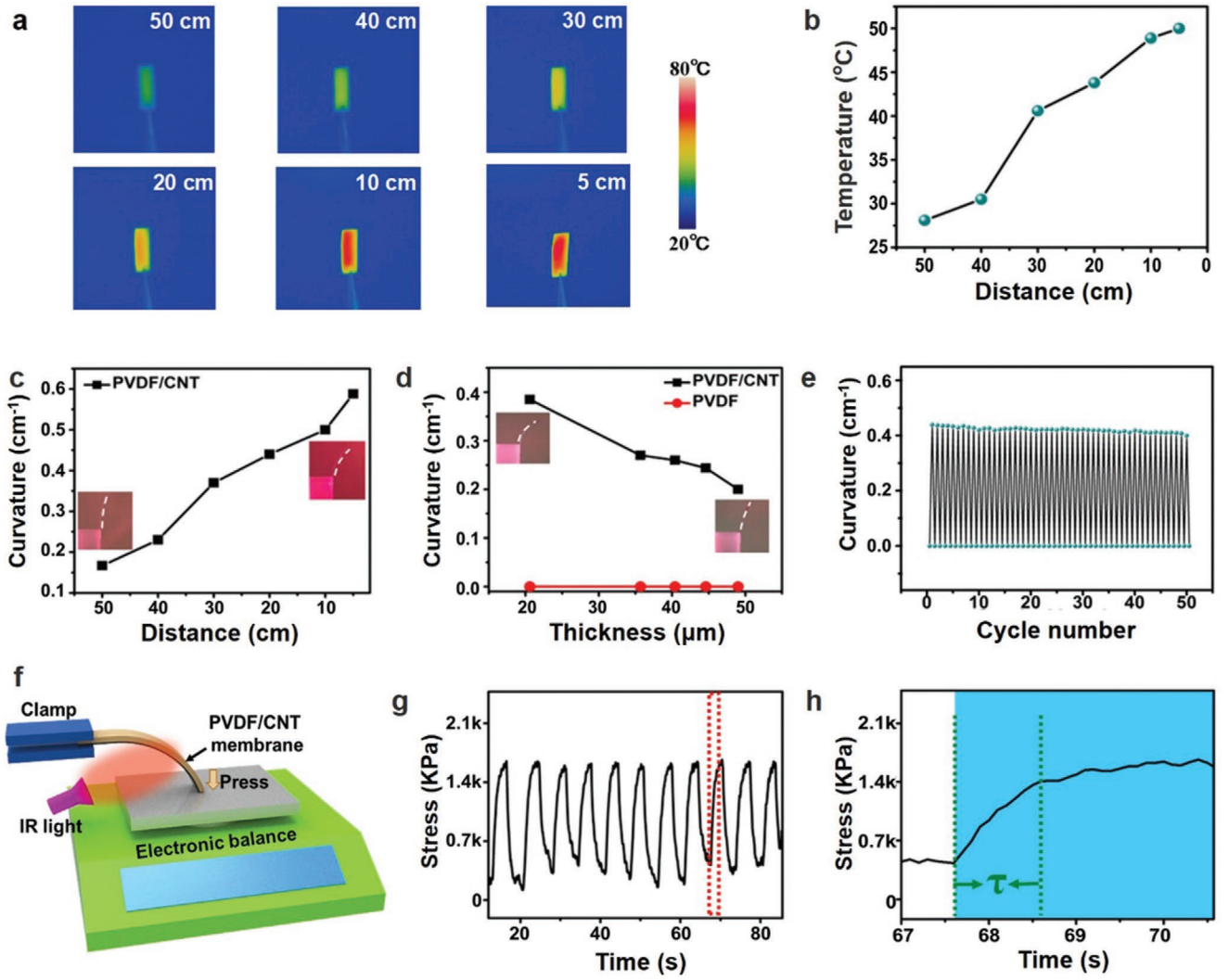

Figure 3. NIR light stimuli responses of the CNTs/PVDF actuator. a) The thermal image, b) surface temperature, and c) bending curvatures of CNTs/PVDF composite when exposed to the light resource from different distances. d) The relationship between bending curvature and the film actuator thickness. e) 50 cycles of light stimuli responsiveness of CNTs/PVDF actuator. f) The schematic illustration of the dynamometer to measure the bending stress of the CNTs/PVDF membrane. g) The stress generated by light-triggered deformation of the CNTs/PVDF actuator in the process of light on/off. h) The magnified curve of the highlighted region in (g).

The CNTs/PVDF membrane was exposed to light irradiation under different distances (from 50 to 5 cm). The CNTs film can convert the NIR light energy into thermal energy, leading to the increasing of the surface temperature of the membrane. The surface temperature of the CNTs/PVDF membrane was monitored by the infrared thermography (**Figure 3**a). With decreasing the distance between the membrane and light resource, the surface temperature of the membrane increases from 28 to 52 °C (Figure 3b). The actuation of a CNT/PVDF stripe (40 μm thickness, 4 × 0.5 cm length × width) under different irradiation distances (from 50 to 5 cm) is shown in Figure 3c. When the light exposes to the side of CNTs film, the CNTs/PVDF membrane bends gradually toward the light resource. The curvature of the CNTs/PVDF membrane increases correspondingly from 0.16 to 0.60 cm^{-1} (Figure 3c). When the light turns off, the membrane returns reversibly to the original upright state. Due to the larger thermal expansion efficiency of PVDF membrane than CNTs film, the photothermal induced volume expansion of PVDF membrane is more apparent than CNTs film,[36] leading the CNTs/PVDF membrane bend toward the CNT film sides.

Except the light stimuli intensity, the thickness of the membrane also influences the actuation behaviors. PVDF membranes with different thicknesses of 20, 35, 40, 45, and 50 μm were prepared to explore the effects of the PVDF membrane thickness on actuation behaviors. The irradiation distance keeps at 20 cm and the generated surface temperature on the membrane is about 44 °C. As the membrane thickness increases from 20 to 50 μm, the curvature of the CNTs/PVDF actuator decreases gradually from 0.4 to 0.2 cm^{-1} (Figure 3d). This actuation curvature variation is mainly scribed to the differences of mechanical strength and thermal transmission of PVDF membranes with different thickness.[37] The PVDF membrane with larger thickness has a higher bending stress and slow thermal transmission, leading to small bending degree.[38]

© 2020 Wiley-VCH GmbH

14392054, 2021, 1, Downloaded from https://onlinelibrary.wiley.com/doi/10.1002/mame.202000502 by Ningbo Institute Of Materials, Wiley Online Library on [12/09/2023]. See the Terms and Conditions (https://onlinelibrary.wiley.com/terms-and-conditions) on Wiley Online Library for rules of use; OA articles are governed by the applicable Creative Commons License

Macromolecular Materials and Engineering
www.mme-journal.de

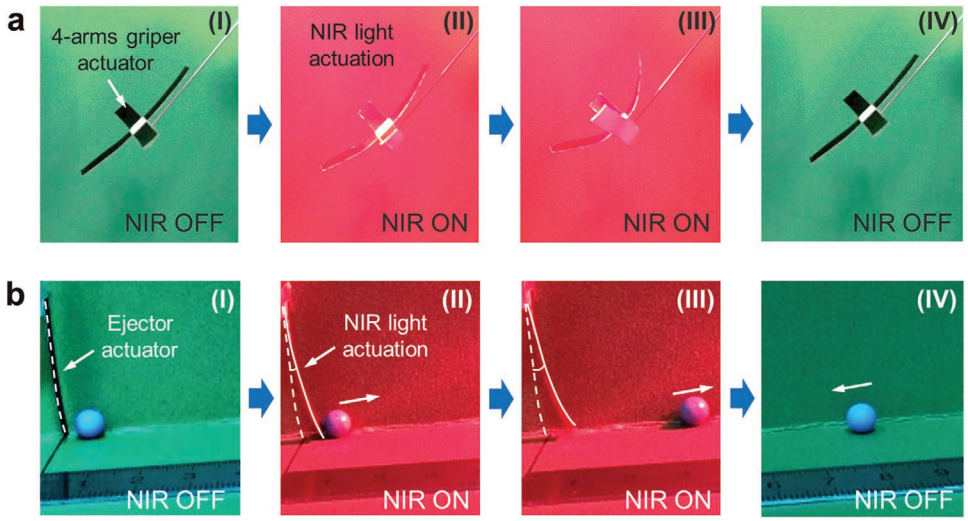

Figure 4. NIR light-driven actuation using CNTs/PVDF bilayer actuator. a) A 4-armed gripper actuator is controlled to open and close under the on/off cyclic NIR irradiation. b) NIR light irradiation-driven ejector that pushes a ball move forward when the NIR light is on and move back when the NIR light is off.

In the repeated on/off light irradiation, the CNTs/PVDF membrane show stable actuation behaviors. After 50 cycles of bending/relaxing, the response speed and maximum bending curvature show no apparent changes and return completely to the original upright state (Figure 3e), indicating outstanding actuation stability. In the process of light stimuli actuation, the bending stress of the CNTs/PVDF membrane was measured by a dynamometer (Figure 3f). A straight CNTs/PVDF stripe with a dimension of 4 × 0.5 cm is held with one end and the other end touches the surface of a flat dynamometer. After exposure to NIR light, the actuator bends generally and presses the dynamometer. The displayed pressure force is used to determine the light-triggered bending stress. The maximum bending stress approach about 1.6 kPa (Figure 3g). Under the light irradiation, the actuator bends rapidly to the equilibrate state within 1 s (Figure 3h).

The potential applications of CNT/PVDF actuators were investigated as a biomimetic gripper and ejector (**Figure 4**). Four individual CNT/PVDF stripes were assembled into a 4-armed gripper (Figure 4a-I). Under the NIR-light irradiation, the four arms bend centripetally at the same time, performing like a closed palm (Figure 4a-II,III). When the NIR light is turned off, the closed gripper opens rapidly (Figure 4a-IV), which can be used potentially as a NIR-controlled gripper to rapidly grab an object. In addition, owing to the rapid NIR-light actuation and large bending stress, the actuator also can serve as a light-driven ejector (Figure 4b). A glass ball with a weight of about 5 g can even be propelled to move forward about 7 cm under NIR light stimuli (Figure 4b-III,IV).

The porous PVDF membrane has strong interaction with volatile organic solvent vapor molecules while the inert CNTs film almost shows no response to them. Because of the different responsiveness of CNTs and PVDF, the double-layer CNT/PVDF membrane deforms asymmetrically to the organic solvent vapor stimuli (**Figure 5**a).[39] A bionic hand-shaped CNTs/PVDF actuator that is responsive to the volatile acetone stimuli was fabricated. To achieve precisely spatial actuation, the acetone vapor was delivered directly by a tube to the targeted finger parts of the hand-shaped actuator. When exposed to the acetone vapor, the finger parts rapidly bend toward the CNTs film sides and reversibly return to the original state upon removing the acetone gas (Figure 5b). PVDF is capable of capturing acetone vapors through noncovalent interactions between fluorine atoms and acetone molecules.[40] In the porous PVDF membrane, acetone vapors molecules diffuse into the membrane and lead to the volume expansion of the PVDF membrane.[41] In addition, acetone vapors has weak interaction with CNTs film. The responsive differences trigger the membrane bend. The responding speeds of CNT/PVDF were investigated by snapshot cameras and the instant screenshots are shown in Figure 5c. As soon as exposure to the acetone vapor, one finger-shaped membrane bends rapidly within 0.19 s. When the acetone vapor is switched off, the bent finger returns to the original straight state in 1.24 s. One reversible bending/relaxing cycle can be finished within 1.43 s. This bending and relaxing speed of prepared CNT/PVDF is much faster than the previous PVDF-based actuator.[7,22,40–47] Compared with other carbon-based PVDF bilayer without porous structures,[11,48] the responding speed of prepared CNT/PVDF is also much faster. The porous structures can accelerate the internal mass transport and give rise to a rapid responsiveness.

As shown in the SEM image (Figure 2b), the prepared PVDF membrane has finger-shaped microscopic pores on one side and small pores are formed on the other sides. Compared with the small porosity, the finger-like pores is favorable for the rapid permeation of acetone molecules, leading to the fast response to the acetone vapor stimuli.[49] A PVDF membrane with small sized pores were prepared as a referenced sample (Figure S1, Supporting Information). Compared with the membrane with larger finger-liked pores (Figure S1a, Supporting Information), the membrane with small-sized pores show slow responding speed and slight deformation under the stimuli of NIR light and acetone. Especially exposing to the acetone vapor, the membrane with small-sized pores hardly display rapid and

© 2020 Wiley-VCH GmbH

14392054, 2021, 1, Downloaded from https://onlinelibrary.wiley.com/doi/10.1002/mame.202000502 by Ningbo Institute Of Materials, Wiley Online Library on [12/09/2023]. See the Terms and Conditions (https://onlinelibrary.wiley.com/terms-and-conditions) on Wiley Online Library for rules of use; OA articles are governed by the applicable Creative Commons License

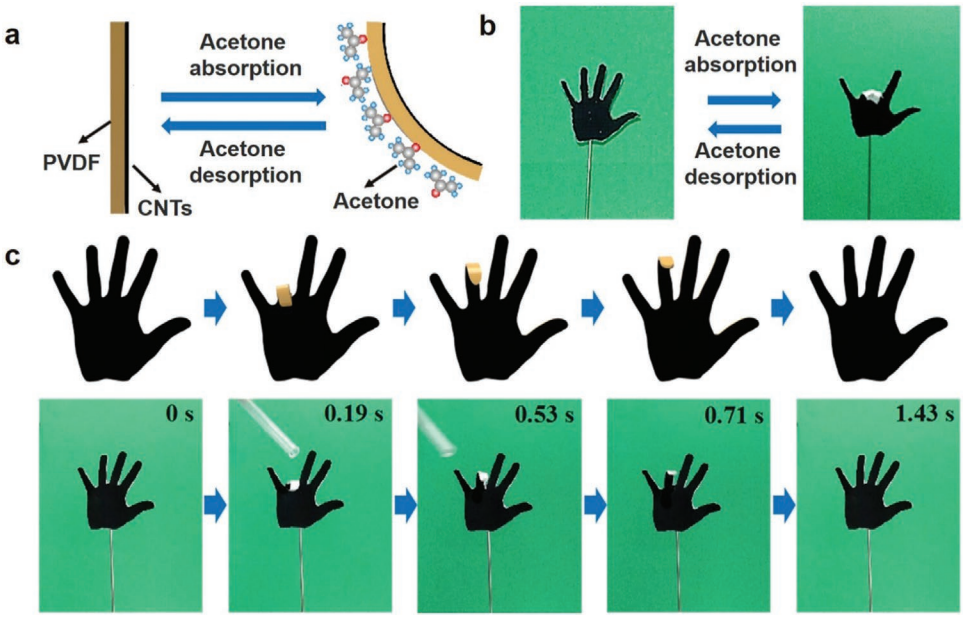

Figure 5. a) The actuation mechanism of the CNTs/PVDF bilayer actuator via solvent molecule absorption/desorption. b) Photos of hand-shaped actuator bending in response to acetone vapors. c) Ultrafast responses of hand-shaped actuator in the presence of acetone vapor stimuli.

apparent deformation (Figure S1b, Supporting Information). These results indicate the porous structure of PVDF membrane plays a crucial role in the performance of the CNTs/PVDF actuator. The asymmetrical pore structures on two sides leads to the asymmetrical distribution of acetone molecules in the membrane, resulting into different volume expansion on the two sides. Therefore, the CNTs/PVDF membrane can bend rapidly toward CNTs film sides.

To demonstrate the responsiveness of CNT/PVDF actuators to other organic solvents, organic solvents including tetrahydrofuran (THF), dichloromethane, diethyl ether, ethanol, and methanol were selected as vapor stimuli. During the vapor actuation, the vapor pressure of the organic solvents was controlled by a pressure gauge and kept around 2 kPa at 20 °C. The CNTs/PVDF membrane with a dimension of 4 × 0.5 cm (length × width) was twisted into a spiral actuator. Upon exposing to the solvent vapors, the actuator uncoils gradually and the length increases correspondingly (**Figure 6**a). Otherwise, the actuator returns to the spiral state when move away from the vapor. To study the deformation behaviors of the actuator to different organic solvents vapors, the length variation of the spiral actuator ($\Delta L/L_0$) is used to evaluate precisely the actuating process (Figure 6a), where L_0, ΔL represent the initial length of the spiral actuator and the length variation after vapor stimuli. Acetone vapor gives rise to the fastest actuating speed and maximum deformation. The spiral actuator uncoils rapidly within 2 s and almost returns to the straight stripe state (Figure 6a). In the case of THF, the spiral actuator only uncoiled partially and the unfold speed was

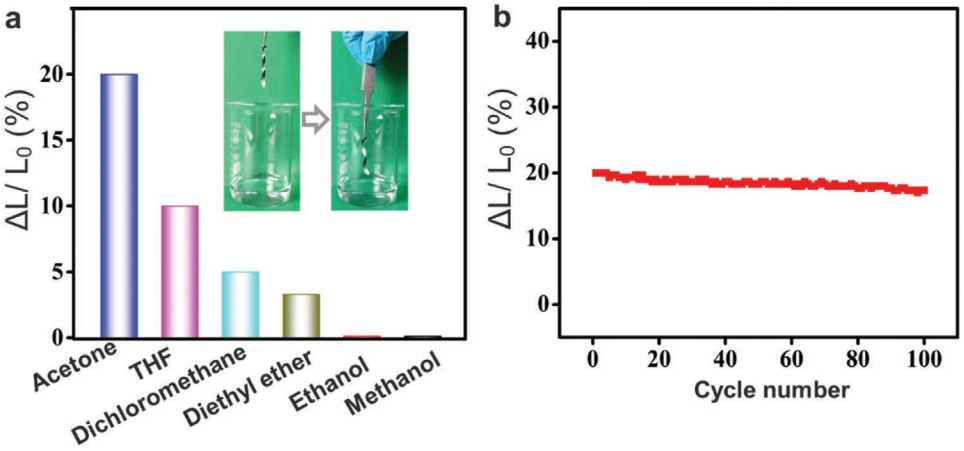

Figure 6. a) The length variation ($\Delta L/L_0$) of spiral actuator under the stimuli of different organic solvent vapors (gas pressure 2 kPa, 20 °C). The inset shows the untwisting of a spiral CNTs/PVDF actuator to acetone vapor stimuli. b) 100 cycles of twisting/untwisting actuations of the CNTs/PVDF spiral actuator.

© 2020 Wiley-VCH GmbH

14392054, 2021, 1, Downloaded from https://onlinelibrary.wiley.com/doi/10.1002/mame.202000502 by Ningbo Institute Of Materials, Wiley Online Library on [12/09/2023]. See the Terms and Conditions (https://onlinelibrary.wiley.com/terms-and-conditions) on Wiley Online Library for rules of use; OA articles are governed by the applicable Creative Commons License

14392054, 2021, 1, Downloaded from https://onlinelibrary.wiley.com/doi/10.1002/mame.202000502 by Ningbo Institute Of Materials, Wiley Online Library on [12/09/2023]. See the Terms and Conditions (https://onlinelibrary.wiley.com/terms-and-conditions) on Wiley Online Library for rules of use; OA articles are governed by the applicable Creative Commons License

also slower than the case of acetone-driven actuation. Other solvents such as ethanol and methanol hardly triggered the deformation of CNT/PVDF actuators (Figure 6a). After 100 cycles of twist/uncoil by acetone vapor stimuli, the $\Delta L/L_0$ value of CNTs/PVDF actuator decreases slightly by 3%, which indicates the CNTs/PVDF actuator has highly reliable actuation behavior and stability to the acetone vapor.

In summary, we develop a bilayer CNTs/PVDF actuator with asymmetrical finger-shaped and small pores structures, which shows fast thermal/acetone responsiveness. The prepared CNTs/PVDF bilayer actuator consisted of macroscopic CNT assembled film and hierarchically porous PVDF membrane. This CNTs/PVDF actuator can sensitively respond to light and acetone vapor stimuli. Especially for acetone, this actuator has an extremely fast response time of 0.19 s. It is considered that the hierarchical porosity consisting of finger-like and small-sized holes are responsible for the rapid responses to acetone. The composite actuator also exhibits excellent actuation durability for up to 100 cycles. This bilayer actuator shows good potential in the application of biomimetic gripper and soft robotics.

Experimental Section

Materials and Characterization: Multiwalled CNTs with an outer diameter of 10–30 nm, a length of 10–30 µm, and over 90 wt% purity and 1.5 wt% COOH group were received from Chengdu Organic Chemistry Co., Ltd. PVDF (6008, Solvay) and DMF were purchased from Sigma-Aldrich. Other chemicals were purchased from Sinopharm Chemical Reagent Co., Ltd. These chemicals were of analytical grade and used as obtained without further purification. Deionized (DI) water was used in all experimental processes.

The prepared flexible membranes were characterized by scanning electron microscopy (Hitachi S4800 scanning microscope) at an acceleration voltage of 4 kV. The WCA measurements were tested at room temperature using an OCA-20 Data Physics instrument. The averaged value of the three results was used to determine the WCA. Plasma treatment of the PVDF surface was performed on a plasma cleaner. The composition of the membrane was characterized by ATR-FTIR spectra using Thermo NICOLET 6700 spectrometer. The Raman spectra of the membrane were recorded using a Renishaw inVia Reflex Raman spectrometer with a 785 nm He-Ne laser resource. A lamp of 100 W infrared bulb was used to provide light stimuli. The light intensity was controlled by changing the distance between the lamp and the sample. The infrared thermal images and temperatures were recorded using an infrared thermometer. The internal stress of the membrane activated by infrared light was studied via a universal testing machine (Instron model 5567).

Preparation of Macroscopic CNTs Thin Films: The macroscopic CNTs thin film was prepared according to the previous reports.[26,50] CNTs (20 mg) were dispersed in the anhydrous ethanol (20 mL) by 1 h consistent sonication to form stable, uniform dispersions. The CNTs dispersion was injected into the water surface by a syringe. Subsequently, upon a compression process by tissue or microporous sponges, a uniform freestanding CNTs monolayer was formed at the solution interface. The resultant CNT film can be transferred stably on other membranes. The size of the CNTs film depends on the surface area of the solution, while the film thickness can be tuned by multiple transferring.

Preparation of Porous PVDF Membrane: PVDF particles (15 g) were added into 85 g DMF in a glass flask. The mixture was then stirred vigorously at 80 °C for 3 h until a homogeneous viscous PVDF/DMF mixture was formed.[51] The resulting mixture was left overnight at room temperature to remove the air bubbles. The PVDF/DMF mixture was subsequently poured onto a clean glass plate and casted in the form of the membrane by blade casting means. The casted PVDF film on the glass plate was immersed subsequently in a large amount of water about 60 s before taking out. The formed membrane was dried in an oven at 60 °C for at least 1 h to remove the DMF solvent. In addition, a PVDF membrane with small sized pores was also prepared as a reference sample. 20 g of PVDF particles were dissolved into 80 g DMF for casting into a film with the same conditions. The film was immersed in the water bath for 10 s before drying.

After cooling to room temperature, the dried PVDF film on a glass plate was exposed to the oxygen plasma for 120 s before peeling off from the substrate.

Preparation of CNTs/PVDF Bilayer Actuator: The plasma-treated PVDF membrane with its hydrophilic surface upside dipped obliquely at an angle of 45° into the solution with CNTs film floating on the surface. Moving slowly toward the beneath of the CNT film, the underlying PVDF membrane was lifted slowly and the CNTs film was transferred to the substrate. The transferring process was repeated to tune the thickness of the CNTs film deposited on the PVDF membrane. After drying at 50 °C for about 1 h, a bilayer CNTs/PVDF composite film was acquired.

Light-Driven Actuation: A 100 W infrared bulb was used as a light stimuli resource to trigger the deformation of the CNT/PVDF actuators. The light intensity was controlled by tuning the distance between the lamp and the membrane. When the CNTs side was exposed to infrared light irradiation, the composite membrane bent toward the light resource. The temperature on the membrane was determined by a thermal infrared camera.

Acetone Vapor-Triggered Actuation: In the spatial selective actuation by acetone vapor, a glass tube linked with a flask containing acetone approached the target position on the CNTs/PVDF composite membrane. The flask was heated at 40 °C to produce continuously acetone vapor. Also, CNTs/PVDF composite membrane was cut into a stripe with 6 cm × 7 mm and put in a beaker containing acetone. The stripe stayed at the position of 3 cm higher above the acetone interface.

Supporting Information

Supporting Information is available from the Wiley Online Library or from the author.

Acknowledgements

The research was supported by the Natural Science Foundation of China (52073295 and 51603219), the Special Fund for Basic Scientific Research of Central Colleges, Chang'an University (Nos. 300102318403 and 300102319306), and the Bureau of Frontier Science and Education of Chinese Academy of Sciences (QYZDB-SSWSLH036) for financial support.

Conflict of Interest

The authors declare no conflict of interest.

Keywords

actuators, carbon nanotubes, multiresponsive actuators, porous polyvinylidene fluoride membranes

Received: August 11, 2020
Revised: October 29, 2020
Published online: November 20, 2020

[1] Y. Dong, J. Wang, X. Guo, S. Yang, M. O. Ozen, P. Chen, X. Liu, W. Du, F. Xiao, U. Demirci, B. F. Liu, *Nat. Commun.* **2019**, *10*, 4087.

© 2020 Wiley-VCH GmbH

[2] P. Xiao, Y. Liang, J. He, L. Zhang, S. Wang, J. Gu, J. Zhang, Y. Huang, S.-W. Kuo, T. Chen, *ACS Nano* **2019**, *13*, 4368.
[3] Y.-C. Cheng, H.-C. Lu, X. Lee, H. Zeng, A. Priimagi, *Adv. Mater.* **2019**, *32*, 1906233.
[4] M. Y. Razzaq, M. Behl, M. Heuchel, A. Lendlein, *Macromol. Rapid Commun.* **2019**, *41*, 1900440.
[5] M. Han, B. Kim, H. Lim, H. Jang, E. Kim, *Adv. Mater.* **2019**, *32*, 1905096.
[6] Y. Liu, F. Zhang, J. Leng, K. Fu, X. L. Lu, L. Wang, C. Cotton, B. Sun, B. Gu, T. W. Chou, *Adv. Mater. Technol.* **2019**, *4*, 1900600.
[7] J. Qu, F. Gao, J. Zhao, L. Duan, Y. Zang, S. Wen, *Smart Mater. Struct.* **2019**, *28*, 105043.
[8] X. Yu, H. Cheng, M. Zhang, Y. Zhao, L. Qu, G. Shi, *Nat. Rev. Mater.* **2017**, *2*, 17046.
[9] Y. Hu, J. Liu, L. Chang, L. Yang, A. Xu, K. Qi, P. Lu, G. Wu, W. Chen, Y. Wu, *Adv. Funct. Mater.* **2017**, *27*, 1704388.
[10] J.-W. Mao, Z.-D. Chen, D.-D. Han, J.-N. Ma, Y.-L. Zhang, H.-B. Sun, *Nanoscale* **2019**, *11*, 20614.
[11] G. Xu, M. Zhang, Q. Zhou, H. Chen, T. Gao, C. Li, G. Shi, *Nanoscale* **2017**, *9*, 17465.
[12] P. Zhou, L. Chen, L. Yao, M. Weng, W. Zhang, *Nanoscale* **2018**, *10*, 8422.
[13] A. Toncheva, B. Willocq, F. Khelifa, O. Douheret, P. Lambert, P. Dubois, J.-M. Raquez, *J. Mater. Chem. B* **2017**, *5*, 5556.
[14] Y. Wang, N. Wu, C. Liu, M. K. Albolkany, M. Wang, Y. Wang, S. Arooj, W. Zhang, B. Liu, *Mater. Horiz.* **2020**, *7*, 149.
[15] L. Chen, M. Weng, P. Zhou, L. Zhang, Z. Huang, W. Zhang, *Nanoscale* **2017**, *9*, 9825.
[16] P. Leeladhar, A. Raturi, J. P. Kumar, Singh, *Smart Mater. Struct.* **2017**, *26*, 095030.
[17] L. Yu, H. Yu, *ACS Appl. Mater. Interfaces* **2015**, *7*, 3834.
[18] J. Zhao, Q. Li, B. Miao, H. Pi, P. Yang, *Small* **2020**, *16*, 2000043.
[19] S. Wang, Y. Gao, A. Wei, P. Xiao, Y. Liang, W. Lu, C. Chen, C. Zhang, G. Yang, H. Yao, T. Chen, *Nat. Commun.* **2020**, *11*, 4359.
[20] X. Zhang, C. L. Pint, M. H. Lee, B. E. Schubert, A. Jamshidi, K. Takei, H. Ko, A. Gillies, R. Bardhan, J. J. Urban, M. Wu, R. Fearing, A. Javey, *Nano Lett.* **2011**, *11*, 3239.
[21] T. Deng, C. Yoon, Q. Jin, M. Li, Z. Liu, D. H. Gracias, *Appl. Phys. Lett.* **2015**, *106*, 203108.
[22] Leeladhar, J. P. Singh, *ACS Appl. Mater. Interfaces* **2018**, *10*, 33956.
[23] L. Zhang, P. Naumov, X. Du, Z. Hu, J. Wang, *Adv. Mater.* **2017**, *29*, 1702231.
[24] W. Wang, C. Xiang, Q. Zhu, W. Zhong, M. Li, K. Yan, D. Wang, *ACS Appl. Mater. Interfaces* **2018**, *10*, 27215.
[25] H. Liu, D. Niu, W. Jiang, T. Zhao, B. Lei, L. Yin, Y. Shi, B. Chen, B. Lu, *Sens. Actuators, A* **2016**, *239*, 45.
[26] L. Zhang, P. Xiao, W. Lu, J. Zhang, J. Gu, Y. Huang, T. Chen, *Adv. Mater. Interfaces* **2016**, *3*, 1600170.
[27] D. M. Correia, J. Nunes-Pereira, D. Alikin, A. L. Kholkin, S. A. C. Carabineiro, L. Rebouta, M. S. Rodrigues, F. Vaz, C. M. Costa, S. Lanceros-Méndez, *Polymer* **2019**, *169*, 138.
[28] M. Kitsara, A. Blanquer, G. Murillo, V. Humblot, S. De Bragança Vieira, C. Nogués, E. Ibáñez, J. Esteve, L. Barrios, *Nanoscale* **2019**, *11*, 8906.
[29] P. Martins, A. C. Lopes, S. Lanceros-Mendez, *Prog. Polym. Sci.* **2014**, *39*, 683.
[30] D. E, G. M. Joshi, K. S, R. R. Deshmukh, S. K. S M, *Prog. Org. Coat.* **2019**, *131*, 17.
[31] C. Xu, F. Yan, M. Wang, H. Yan, Z. Cui, J. Li, B. He, *J. Membr. Sci.* **2020**, *602*, 117974.
[32] A. Kaynak, T. Mehmood, X. J. Dai, K. Magniez, A. Kouzani, *Materials* **2013**, *6*, 3482.
[33] F. Yalcinkaya, A. Siekierka, M. Bryjak, *RSC Adv.* **2017**, *7*, 56704.
[34] V. Dhand, S. K. Hong, L. Li, J.-M. Kim, S. H. Kim, K. Y. Rhee, H. W. Lee, *Composites, Part B* **2019**, *160*, 632.
[35] S. Al-Gharabli, J. Kujawa, M. O. Mavukkandy, T. A. Agbaje, E. M. Hamad, H. A. Arafat, *Eur. Polym. J.* **2018**, *100*, 153.
[36] Y. Tai, G. Lubineau, Z. Yang, *Adv. Mater.* **2016**, *28*, 4665.
[37] E. Sachyani, M. Layani, G. Tibi, T. Avidan, A. Degani, S. Magdassi, *Sens. Actuators, B* **2017**, *252*, 1071.
[38] D. K. Seo, T. J. Kang, D. W. Kim, Y. H. Kim, *Nanotechnology* **2012**, *23*, 075501.
[39] D. H. Ho, S. Cheon, P. Hong, J. H. Park, J. W. Suk, D. H. Kim, J. T. Han, J. H. Cho, *Adv. Funct. Mater.* **2019**, *29*, 1900025.
[40] J. Wei, F. Wang, L. Zhang, *ACS Appl. Mater. Interfaces* **2018**, *10*, 29161.
[41] Y. Yuan, J. Yuan, H. Tan, X. Song, Y. Tu, T. Zhang, H. Han, W. Huang, X. Huang, L. Zhang, *Macromol. Mater. Eng.* **2019**, *304*, 1800501.
[42] H. Tan, S. Liang, X. Yu, X. Song, W. Huang, L. Zhang, *J. Mater. Chem. C* **2019**, *7*, 5410.
[43] H. Shen, J. Ding, N. Yuan, J. Xu, L. Han, X. Zhou, B. Fang, *J. Inorg. Organomet. Polym. Mater.* **2018**, *28*, 1962.
[44] J. Wei, X. Qiu, L. Zhang, *ACS Appl. Mater. Interfaces* **2019**, *11*, 16252.
[45] Y. Jin, Q. Zhu, W. Zhong, K. Yan, D. Wang, *J. Phys. Chem. C* **2019**, *123*, 185.
[46] S. Liang, X. Qiu, J. Yuan, W. Huang, X. Du, L. Zhang, *ACS Appl. Mater. Interfaces* **2018**, *10*, 19123.
[47] Y. He, Q. Chen, H. Liu, L. Zhang, D. Wu, C. Lu, W. OuYang, D. Jiang, M. Wu, J. Zhang, Y. Li, J. Fan, C. Liu, Z. Guo, *Macromol. Mater. Eng.* **2019**, *304*, 1970018.
[48] Y.-L. Zhang, J.-N. Ma, S. Liu, D.-D. Han, Y.-Q. Liu, Z.-D. Chen, J.-W. Mao, H.-B. Sun, *Nano Energy* **2020**, *68*, 104302.
[49] Q. Zhao, J. W. C. Dunlop, X. Qiu, F. Huang, Z. Zhang, J. Heyda, J. Dzubiella, M. Antonietti, J. Yuan, *Nat. Commun.* **2014**, *5*, 4293.
[50] L. Zhang, Y. Tao, P. Xiao, L. Dai, L. Song, Y. Huang, J. Zhang, S.-W. Kuo, T. Chen, *Adv. Mater. Interfaces* **2017**, *4*, 1601105.
[51] S. J. Oh, N. Kim, Y. T. Lee, *J. Membr. Sci.* **2009**, *345*, 13.

© 2020 Wiley-VCH GmbH

14392054, 2021, 1, Downloaded from https://onlinelibrary.wiley.com/doi/10.1002/mame.202000502 by Ningbo Institute Of Materials, Wiley Online Library on [12/09/2023]. See the Terms and Conditions (https://onlinelibrary.wiley.com/terms-and-conditions) on Wiley Online Library for rules of use; OA articles are governed by the applicable Creative Commons License